PROCEEDINGS OF SCIENCE

On gamma rays as predictors of UHECR flux in AGNs

Cainã de Oliveira,[a,*] **Rodrigo Guedes Lang**[b] **and Pedro Batista**[b]

[a] *Instituto de Física de São Carlos, Universidade de São Paulo, Av. Trabalhador São-carlense 400, São Carlos, Brasil*

[b] *Friedrich-Alexander-Universität Erlangen-Nürnberg, Erlangen Centre for Astroparticle Physics, Nikolaus-Fiebiger-Str. 2, 91058 Erlangen, Germany*

E-mail: caina.oliveira@usp.br, rodrigo.lang@fau.de, pedro.batista@fau.de

Active galactic nuclei (AGNs) are significant candidates for ultra-high-energy cosmic ray (UHECR) sources, supported by both theoretical and phenomenological motivations. In this context, AGN catalogs have been employed for quantitative comparisons between predictions and observations, where the UHECR flux is assumed to be proportional to the very-high-energy γ-ray flux of the objects. However, discrepancies arise in matching the energy spectrum and anisotropy data. This work proposes a possible solution to these inconsistencies. By using the observed γ-ray flux as a proxy for the UHECR flux, a beamed UHECR emission is implicitly assumed. We show that assuming isotropic UHECR emission and applying Doppler factor corrections to the observed γ-ray flux can reduce the discrepancies between the predictions derived from AGN catalog-based models.

7th International Symposium on Ultra High Energy Cosmic Rays (UHECR2024)
17-21 November 2024
Malargüe, Mendoza, Argentina

*Speaker

 ISSN 1824-8039 . Published by SISSA Medialab.

PoS(UHECR2024)079

1. Introduction

The origin of ultra-high-energy cosmic rays (UHECR) remains one of the greatest mysteries of contemporary astrophysics [1]. As charged particles, their trajectories are deflected by extragalactic and galactic magnetic fields, preventing the direct identification of their astrophysical sources. In the last years, measurements from the Pierre Auger [2] and Telescope Array [3] Observatories have significantly advanced our understanding of cosmic rays in the ultra-high-energy range. In particular, the detection of a dipolar modulation of events with energies exceeding 8 EeV provides strong evidence for the extragalactic origin of these particles [4]. Furthermore, the observation of smaller-scale anisotropies in the UHECR sky at higher energies ($\sim$ 40 EeV) has enabled correlation studies between arrival direction data and various catalogs of astrophysical objects [5, 6].

Active Galactic Nuclei (AGN) and Starburst Galaxies (SBGs) have been considered suitable candidates of UHECR sources. A reported correlation between data from the Pierre Auger Observatory and a catalog of nearby SBG achieved a confidence level of 4.2σ [5], which increased to 4.7σ when combined with data from the Telescope Array [6]. In comparison, the Pierre Auger Collaboration reported a correlation of 3.3σ confidence level for a catalog of nearby AGN [5].

AGNs are considered compelling candidates for UHECR sources, supported by both theoretical and phenomenological arguments [7]. Different sites have been proposed as UHECR accelerators, including the vicinity of the supermassive black hole, the jet (on parsec and kiloparsec scales), the backflow of jet material, the jet termination shock, and the lobes. Among AGNs, radio galaxies have demonstrated significant potential in explaining the energy spectrum, composition, and arrival direction data. The three brightest nearby radio galaxies, Centaurus A, M87, and Fornax A, may account for the highest-energy dipole and hotspots observed [8, 9].

According to the unified model of AGNs, radio galaxies and blazars are jetted AGNs whose jets are misaligned and aligned, respectively, with our line of sight. Consequently, if radio galaxies are dominant UHECR sources, blazars must also contribute to the UHECR flux. Nevertheless, combining radio galaxies and blazars in AGN catalogs results in poor agreement between model predictions and observational data [10, 11]. The contribution of the blazar Mkn 421 produces a strong hotspot and dominates the dipole direction, while distant blazars increase the number of secondary particles. UHECR accelerated by farther sources undergoes more photodisintegration, increasing the number of secondary particles, which deteriorates the fit quality of the energy spectrum. When an astrophysical catalog is used to predict the UHECR signal, assumptions must be made about the individual UHECR luminosity of the sources. In the case described above, the observed γ-ray luminosity is used to weigh the contribution of each source.

In this work, we propose a possible solution to the tension between the data and the combined predictions for radio galaxies and blazars. UHECRs emitted by AGNs are unlikely to remain collimated, as is the case for γ rays emitted along AGN jets. We show that assuming isotropic emission for UHECRs can reduce the discrepancies between UHECR predictions based on AGN catalogs and the data.

2. Gamma rays and cosmic rays from jetted AGNs

The detection of γ rays from AGNs indicates the presence of regions of particle acceleration [12]. It is typically assumed that electrons/positrons or protons are accelerated in compact regions moving at relativistic speeds along the jet (*blobs*). In the blob's rest frame, the accelerated particles will emit γ rays isotropically. For an external observer, however, the radiation is highly beamed within an angle $\theta_b \approx \Gamma_b^{-1}$, where Γ_b is the bulk Lorentz factor. In this scenario, the luminosity attributed to the source (observed, L_γ^{obs}) is boosted by a factor of $\mathcal{D}^4$ compared to the intrinsic luminosity determined in the source's rest frame (L_γ^{int}). The Doppler factor $\mathcal{D}$ is given by $\mathcal{D}^{-1} = \Gamma_b(1 - \beta_b \cos\theta)$, where β_b is the plasma speed in units of the speed of light, and θ is the angle between the jet axis and the observer's line of sight [13].

Different mechanisms and sites have been proposed for accelerating UHECRs in AGN jets. In the case of UHECRs being accelerated in relativistic plasmas, it is expected that they will experience the same beaming effect observed for γ rays. However, as charged particles, UHECRs are likely to become isotropized within the source region. In a detailed study [14], it was found that the angular distribution of accelerated UHECRs along the jet is determined by deflections within the cocoon. Even in the more anisotropic scenarios proposed in their work, only about half of the particles were emitted collimated within an angle larger than θ_b.

After escaping the acceleration site, the UHECRs should cross the lobes inflated by the AGN's jet before reaching the extragalactic medium. The extension of the lobes is about $R \sim 100$kpc, with possibly turbulent/filamentary magnetic fields of intensity $\sim 1-10\mu$G [15, 16]. In this environment, the UHECRs will have a scattering length approximately given by [17] $\lambda_s \sim \kappa^2 \ell_c (r_L/\ell_c)^\delta$, where $\kappa = B_0^2/\delta B^2$, ℓ_c is the magnetic field coherence length, δ is the diffusion coefficient, r_L is the gyroradius of the UHECR. B_0 and δB are the large-scale and turbulent components of the magnetic field, respectively. For $\ell_c \sim 0.1R$, and the fiducial value $\kappa \approx 1$, it is possible to estimate that all particles with energies below $E_s \sim (Z \times 30\ \text{EeV}) B_{\mu G} \sqrt{\ell_{10} R_{100}}$[1] will suffer at least one scattering inside the lobe, losing it directional information. For the estimation above, we use the conservative value $\delta = 2$, which is appropriate for the high-energy non-resonant regime [18]. Above 5 EeV, the UHECR detected on Earth are dominated by He and N, as inferred from the combined fit performed by the Pierre Auger Collaboration [19]. Taking $Z \sim 5$, we estimate $E_s \sim 150$ EeV, suggesting that all UHECRs are likely scattered before leaving the source's vicinity.

The estimation above assumes that the UHECRs are accelerated in shocks at the first parsec scales from the jet base. However, scattering may be inefficient if the acceleration primarily takes place in the termination shocks of the jets. It has been argued that these sites are poor UHECR accelerators when considering shock acceleration [20], though a cavity behind the termination shock could serve as an important accelerator site [21].

It is unlikely that the UHECR remains beamed after leaving the source region, as is the case for γ rays. Thus, using the observed γ-ray luminosity as a proxy for UHECR luminosity may overestimate the latter by a factor of $\mathcal{D}^q$, where q accounts for the γ ray/UHECR association. For example, if the UHECR luminosity scales with L_γ^{int}, then $q = 4$ [13]. Assuming the UHECR luminosity scales with the radiative jet power, $q = 2$ [22]. This effect is particularly important when AGNs of different classes are included in the same analysis. Radio galaxies have a mean Doppler

[1] with $\ell_{10} = \ell_c/10$ kpc, $R_{100} = R/100$ kpc, and $B_{\mu G} = B_0/1\ \mu$G.

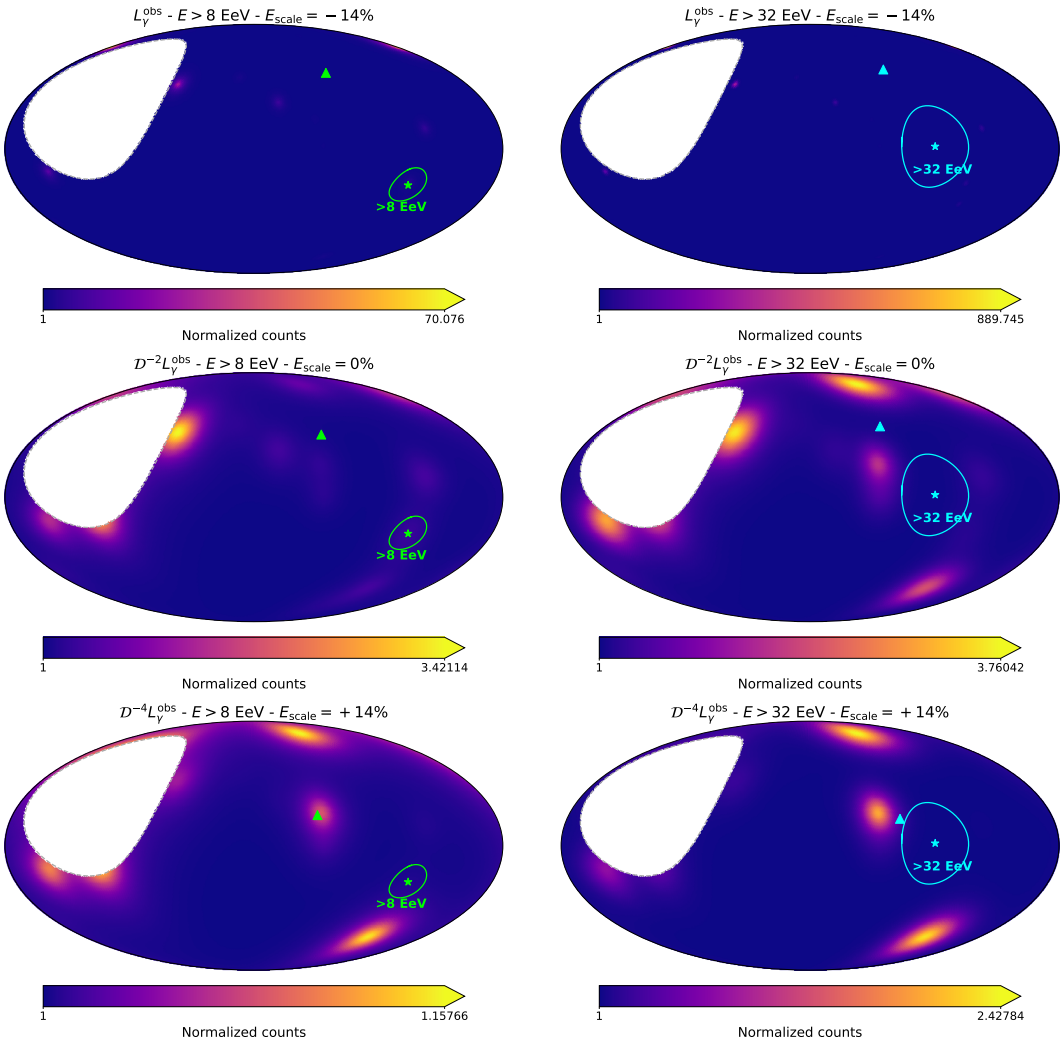

Figure 1: Arrival direction maps and reconstructed dipole directions obtained for the best-fit scenario considering each of the γ-ray proxies (rows) for $E > 8$ EeV (left) and $E > 32$ EeV (right). The counts are normalized to the bin with the fewest counts. The lime and cyan stars and contours show the dipole measured by the Pierre Auger Observatory for $E > 8$ eV and $E > 32$ eV. Triangles show the obtained dipoles the Auger field of view. The data is shown only for the Auger's field of view.

factor $\mathcal{D} \sim 2.6$, while BL Lac (BLL) blazars have $\mathcal{D} \sim 10$ [23, 24]. As a result, the UHECR flux from BLL can be overestimated by a factor of $\sim 15 - 200$ compared to radio galaxies.

3. Effects on the combined fit

To verify the importance of the relativistic beaming effect in AGN scenarios, a combined fit of the energy spectrum and composition was performed, similar to that of [10]. Two classes of sources were considered: a homogeneous distribution of identical background sources (without source evolution) and local point sources. The local sources correspond to the objects in the γAGN catalog proposed by [10]. The catalog contains jetted AGNs detected by the Fermi-LAT satellite [25], with

fluxes exceeding $3.3 \times 10^{-11}\mathrm{cm}^{-2}\mathrm{s}^{-1}$ in the energy range from 10 GeV to 1 TeV. The emissivity of the local sources is considered proportional to: a) the observed γ-ray luminosity (L_γ^{obs}), b) the radiative power of the jet ($\mathcal{D}^{-2}L_\gamma^{obs}$), and c) the intrinsic γ-ray luminosity ($\mathcal{D}^{-4}L_\gamma^{obs}$). The sources and their properties are described in Table 1. The relative contribution of the local and background sources is given by the parameter α, which is the ratio of their fluxes at $10^{19.5}$ eV.

The sources are assumed to emit an effective energy spectrum given by

$$\frac{dN}{dE}(E) = N_s F_i E^{-\Gamma} f_{cut}(E, Z_i, R_{max}), \tag{1}$$

for a normalization N_s, spectral index Γ, and maximum rigidity at the source R_{max}. $F_i = f_i(Z_i R_{max})^{\Gamma-1}$ is the total contribution of a primary i with charge Z_i between 1 EeV and $Z_i R_{max}$.

The unidimensional propagation of five representative primaries (^{1}H, ^{4}He, ^{14}N, ^{28}Si, ^{56}Fe) with energies between 10^{18} and 10^{22} eV (10 bins per decade) was simulated using `CRPropa3` [26]. The particles were emitted from distances ranging from 3 to 3342 Mpc (118 bins in log). All interactions and energy losses were considered for the CMB and EBL model of [27]. The simulations do not account for magnetic field effects. A smearing in the arrival directions was considered by applying a rigidity-dependent von Mises-Fisher distribution with $\Delta_0 = 5°$ and $R_0 = 10$ EV[2]. The simulated results were fitted to the spectral data[28] ($> 10^{18.7}$ eV), and to the first and second moments of the X_{max} distribution[29]. The EPOS-LHC hadronic model [30] was considered. By minimizing the χ^2 distance between the model and the data, the values of the free parameters F_i, N_s, α, Γ, and R_{max} were obtained. To address the systematic uncertainties in the spectrum and X_{max}, additional fits were performed with the energy and X_{max} data shifted by ±14% and 1σ, respectively. The best fit for cases a), b), and c) was obtained for energy shifts of −14%, 0%, and +14%, respectively, with no X_{max} shift.

The values of χ^2/NDF obtained for the models are 4.6, 3.1, and 3.9 for cases a), b), and c), respectively. This indicates an improvement in the fit quality for the new proposed proxies compared to L_γ^{obs} (case a).

Figure 1 shows the arrival direction maps and the reconstructed dipole for $E > 8$ EeV and $E > 32$ EeV. The dipole directions obtained in each case for the field of view of the Pierre Auger Observatory are also shown. The angular distance between the reconstructed and measured dipoles by the Pierre Auger Observatory [4] above 8 EeV (32 EeV) is: a) 5.9σ (2.1σ), b) 4.9σ (2.0σ), and c) 3.5σ (1.1σ). The tension between the Auger dipole and the modeled dipole direction is reduced for the new proxies. The amplitude of the dipole in the model (> 8 EeV) is: a) 14 ± 1%, b) 7.5 ± 0.2%, and c) 4.1 ± 0.5%. When compared to the amplitude of $7.4^{+1.0}_{-0.2}$% reported by the Pierre Auger Collaboration[4], the new proxies significantly improve the agreement between the model and the data.

The hotspots also vary in the different scenarios considered. For L_γ^{obs} (case a), Mkn 421 is the dominant source, producing a spurious hotspot and dominating the dipole direction. For $\mathcal{D}^{-2}L_\gamma^{obs}$ and $\mathcal{D}^{-4}L_\gamma^{obs}$ (cases b and c), the nearby radio galaxies Cen A, M87, and Fornax A dominate within the Auger field of view.

[2] See eq. 2.14 of [10]

4. Summary

In this work, we propose using intrinsic source properties, such as intrinsic γ-ray luminosity or radiative jet power, rather than observed γ-ray luminosity as a proxy for the UHECR luminosity in AGNs. These new proxies are based on the relativistic beaming that the γ-rays are subject. On the other hand, even if emitted beamed, the UHECR must be isotropized within the source region. This effect is particularly important when populations of radio galaxies and blazars are considered in the same analysis. Since blazars have higher Doppler factors compared to radio galaxies, the UHECR flux from them is significantly overestimated relative to radio galaxies. This overestimation increases the contribution of distant sources to the energy spectrum, which worsens the fit. In particular, the high Doppler factor of Mkn 421 causes this blazar to dominate the UHECR sky in models considering the L_γ^{obs} proxy.

When comparing the combined fit results for models based on L_γ^{obs}, $\mathcal{D}^{-2}L_\gamma^{obs}$, and $\mathcal{D}^{-4}L_\gamma^{obs}$, the new proxies improve the fit quality from $\chi^2/NDF = 4.6$ to $\chi^2/NDF = 3.1$. The dipole amplitude decreases from 14% to 4.1 – 7.5%, reducing the tension with the data (7.4%). The predicted dipole direction tension is reduced from 5.9 $(2.1)\sigma$ to 3.5 $(1.1)\sigma$ when compared to the one measured by the Pierre Auger Observatory above 8 EeV (32 EeV). Note that we did not consider extragalactic and galactic magnetic fields in this study.

Finally, this work strengthens the hypothesis of AGNs as candidates for UHECR sources, providing a more robust connection between UHECR and γ-ray luminosities. These assumptions could be applied in future studies to further test AGN scenarios for the origin of UHECR.

References

[1] R. Alves Batista et al., *Front. Astron. Space Sci.* **6** (2019) .

[2] The Pierre Auger Collaboration, *Nucl. Instrum. Methods Phys. Res. A* **798** (2015) 172.

[3] T. Abu-Zayyad et al., *Nucl. Instrum. Methods Phys. Res. A* **689** (2012) 87.

[4] A. Abdul Halim et al., *The Astrophysical Journal* **976** (2024) 48.

[5] P. Abreu et al., *The Astrophysical Journal* **935** (2022) 170.

[6] A. di Matteo et al. for the Pierre Auger and Telescope Array collaborations, *EPJ Web Conf.* **283** (2023) 03002.

[7] F.M. Rieger, *Universe* **8** (2022) .

[8] J. H. Matthews et al., *Mon. Not. R. Astron. Soc. Lett.* **479** (2018) L76.

[9] C. de Oliveira and V. de Souza, *The Astrophysical Journal* **925** (2022) 42.

[10] A. Abdul Halim et al., *Journal of Cosmology and Astroparticle Physics* **2024** (2024) 022.

[11] A. Partenheimer et al., *The Astrophysical Journal Letters* **967** (2024) L15.

[12] R. Blandford et al., *Annual Review of Astronomy and Astrophysics* **57** (2019) 467.

AGN	Class	(RA, DEC) (°)	Distance (Mpc)	$F_{3fhl}/10^{-12}$[a]	$\mathcal{D}$	Ref.[b]
CenA	RG	(201.37, -43.02)	3.68	7.41	1.0	[24]
M87	RG	(187.71, 12.39)	16.7	9.55	1.3	[24]
FornaxA	RG	(50.67, -37.21)	20.4	2.59	1.0	[24]
CenB	RG	(206.7, -60.41)	55.2	2.12	2.3	[24]
NGC1275	RG	(49.95, 41.51)	78.0	47.97	7.5	[24]
IC310	RG	(49.18, 41.32)	83.2	6.90	1.9	[24]
TXS0149+710	BCU	(28.36, 71.25)	103.3	3.72	2.2	[24]
NGC1218	RG	(47.11, 4.11)	124.7	2.42	3.4	[24]
Mkn421	BLL	(166.1, 38.21)	133.7	437.47	14.5	[23]
Mkn501	BLL	(253.47, 39.76)	152.1	156.19	5.7	[23]
TXS0128+554	BCU	(22.81, 55.75)	162.9	0.99	5.1	C23
CGCG050-083	BCU	(235.89, 4.87)	178.6	3.60	5.1	C23
1RXSJ022314.6-111741	BLL	(35.81, -11.29)	182.8	1.24	4.8	C23
1ES2344+514	BLL	(356.76, 51.69)	196.8	30.74	2.7	[31]
PMNJ0816-1311	BLL	(124.11, -13.2)	200.4	16.07	5.9	C23
Mkn180	BLL	(174.11, 70.16)	203.2	15.25	1.4	[31]
1ES1959+650	BLL	(299.97, 65.16)	211.8	67.74	7.3	C23
SBS1646+499	BLL	(251.9, 49.83)	212.8	1.89	5.8	[31]
APLibrae	BLL	(229.42, -24.37)	216.8	20.33	7.1	C23
TXS0210+515	BLL	(33.55, 51.77)	218.8	6.21	5.4	C23
3C371	BLL	(271.71, 69.82)	225.9	4.29	4.0	[23]
PKS1349-439	BLL	(208.24, -44.21)	228.0	0.87	5.7	C23
1RXSJ020021.0-410936	BLL	(30.09, -41.16)	234.4	2.72	4.9	C23
PKS0625-35	BLL	(96.78, -35.49)	238.8	12.38	6.8	[24]
1ES2037+521	BLL	(309.85, 52.33)	238.8	3.72	5.5	C23
PKS0521-36	BLL	(80.76, -36.46)	241.0	5.52	7.0	C23

[a] Energy Flux from Fermi 3FHL catalog (10 GeV - 1 TeV), in erg cm^{-2} s^{-1}, https://heasarc.gsfc.nasa.gov/W3Browse/fermi/fermi3fhl.html

[b] C23 corresponds to $\mathcal{D}^{-2} = -0.21 \log L^{iso} + 7.67$ from [32]

Table 1: Relevant data for the AGNs used in the analysis.

[13] C.D. Dermer and G. Menon, *High energy radiation from black holes: gamma rays, cosmic rays, and neutrinos*, Princeton Series in Astrophysics (2009).

[14] R. Mbarek and D. Caprioli, *The Astrophysical Journal* **886** (2019) 8.

[15] M.J. Hardcastle and M.G.H. Krause, *Mon. Not. R. Astron. Soc.* **443** (2014) 1482.

[16] S. Wykes et al., *Mon. Not. R. Astron. Soc.* **442** (2014) 2867.

[17] R. G. Lang et al., *Phys. Rev. D* **102** (2020) 063012.

[18] N. Globus et al., *A&A* **479** (2008) 97.

[19] A. Abdul Halim et al., *Journal of Cosmology and Astroparticle Physics* **2024** (2024) 094.

[20] A. T. Araudo et al., *Mon. Not. R. Astron. Soc.* **473** (2017) 3500.

[21] B. Cerutti and G. Giacinti, *A&A* **676** (2023) A23.

[22] Y. Chen et al., *The Astrophysical Journal Supplement Series* **265** (2023) 60.

[23] L. Zhang et al., *The Astrophysical Journal* **897** (2020) 10.

[24] X.-H Ye et al., *Publications of the Astronomical Society of the Pacific* **135** (2023) 014101.

[25] M. Ajello et al., *The Astrophysical Journal Supplement Series* **232** (2017) 18.

[26] R. A. Batista et al., *Journal of Cosmology and Astroparticle Physics* **2016** (2016) 038.

[27] R. C. Gilmore et al., *Mon. Not. R. Astron. Soc.* **422** (2012) 3189.

[28] Pierre Auger collaboration, *PoS* **ICRC2019** (2020) 450.

[29] Pierre Auger collaboration, *PoS* **ICRC2019** (2020) 482.

[30] T. Pierog et al., *Phys. Rev. C* **92** (2015) 034906.

[31] L. Chen, *The Astrophysical Journal Supplement Series* **235** (2018) 39.

[32] Y. Chen et al., *Mon. Not. R. Astron. Soc.* **519** (2023) 6199.